Hydrocarbon Production and Microseismic Monitoring – Treatment Optimization in the Marcellus Shale*

Carl W. Neuhaus[1], Cherie Telker[2], Mary Ellison[2], and Keith Blair[3]

Search and Discovery Article #80310 (2013)
Posted August 26, 2013

*Adapted from extended abstract prepared in conjunction with oral presentation at AAPG Annual Convention and Exhibition, Pittsburgh, Pennsylvania, May 19-22, 2013, AAPG©2013

[1]MicroSeismic, Inc. (cneuhaus@microseismic.com)
[2]MicroSeismic, Inc.
[3]Gastar Exploration, Ltd.

Abstract

An integrated analysis of hydraulic fracturing treatments in the Marcellus Shale monitored by a permanently installed array of buried geophones was conducted to investigate the relationship between reservoir geology, wellbore completion and stimulation design, and microseismic data. Available data from other sources (such as well logs and well cores, information on reservoir properties, regional and local geology, and other sub-surface structural information) was utilized to determine how factors related to the specific geology in the Marcellus and to the variability of hydraulic fracture treatments impacted the microseismic response of the formation. These findings were then used to evaluate the correlation between hydrocarbon production and microseismic results relative to changes in geology and variability of the stimulation approach. The observed variability in the microseismic response under the footprint of the array was used to derive and extrapolate regional trends to optimize field development. The initial production was compared to reservoir and engineering parameters, such as treatment pressures, sequence of treatments (toe-to-heel vs. zipper-frac), net pressures, and stage spacing, to determine if the variability in the microseismic results is due to engineering differences or to spatially-varying reservoir properties.

A stress inversion based on focal mechanisms was used to explain the asymmetry of the microseismicity about the wellbore and calculate the magnitudes and directions of the three principal stresses. Fracture orientations defined by failure planes from source mechanisms were used to build a discrete fracture network (DFN) representing the existing unstimulated fracture network in the Marcellus Shale. Simulations then calculated where failure is likely to occur in the DFN during the stimulation using data obtained from the stress inversion comparing the results to the microseismic event locations. Finally, a calibrated model was used to determine the effect of changes in treatment parameters, such as flow rate, treatment pressure, and volume of fluid pumped as well as completion parameters such as stage length, number of perforations, and perforation cluster spacing, in order to optimize the hydraulic fracturing design.

Introduction

Microseismic monitoring of hydraulic fracturing treatments of unconventional reservoirs has become an accepted industry practice and standard in the last decade. Especially in shales, the fracture created during hydraulic stimulation greatly deviates from the planar bi-wing textbook example that has been an accepted image in the industry for a long time. In these heavily fractured ultra-low permeability reservoirs the fracture network is highly complex; accurate imaging of this network is therefore a prerequisite to understanding the response of the formation to the treatment as well as the effect of the treatment on production in order to optimize the wellbore completion and the stimulation treatment (Neuhaus et al., 2012).

Neuhaus et al. (2012) showcased an integrated analysis of microseismic data acquired during the hydraulic fracturing treatment of altogether five wellpads completed in the Marcellus Shale. The case study provided a detailed investigation of the microseismic data in conjunction with other data, such as well logs and cores, reservoir properties, and information on regional and local geology. It determined how factors related to the geology of the reservoir and to the stimulation approach impacted the microseismic results. These observations were then used to relate changes in the microseismicity, changes in the geology, and changes in the stimulation method to changes in production. Utilizing these initial results, a calibrated model was used to determine the effect of changes in treatment parameters, such as flow rate, treatment pressure, and volume of fluid pumped as well as completion parameters such as stage length, number of perforations, and perforation cluster spacing, in order to optimize the hydraulic fracture design.

Data Set

The microseismic data set used in this publication was acquired with a permanently-installed near- surface array consisting of 101 geophones, as seen in Figure 1. To ensure optimal coupling with the earth, the geophones are cemented in place in purpose-drilled shallow boreholes. In principal, similar to a dish microphone, surface microseismic monitoring utilizes full waveform stacking to determine microseismic hypocenters. The array of geophones, representing the dish, can be computationally pointed at target locations, which is referred to as beamstearing, a type of migration commonly used in conventional seismic imaging. The wide azimuth, large-aperture, and high fold geometry allows for a consistent resolution under the entire footprint of the array, in this case covering an area of just over 18 square miles. Stacking hundreds to thousands of seismic traces drastically enhances the signal-to-noise ratio allowing for an accurate estimate of the hypocenter location. The wide azimuth and large aperture sampling of the seismic wavefront provides a high-confidence estimate of event magnitude as well as the failure mechanism for every event (Duncan and Williams-Stroud, 2009; Neuhaus et al., 2012).

Geology

The middle Devonian Marcellus Shale covers more than 34 million acres in New York, Pennsylvania, Ohio, and West Virginia (Engelder et al., 2009). The Marcellus Shale is the lower unit of the Hamilton Group and can be divided into two members: the Upper Marcellus or Oatka Creek and the Lower Marcellus or Union Spring which contains more than 10% TOC. Overlying the Marcellus Shale is the Mahantango or Skaneateles Formation which is an inorganic shale. The Marcellus Shale conformably overlies the Onesquethaw Group which consists of the

limestone, chert, and inorganic shale, including the Onondaga Limestone. During the Devonian, the Acadian Orogeny was simultaneously building the Acadian Mountains and deepening the adjacent foreland basin. Erosion from the Acadian Mountains contributed to the terrigenous material deposited in the foreland basin as the Hamilton Group. The Marcellus Shale was deposited as a thick wedge of fine-grained organic-rich mud on top of the drowned carbonates that form the Onondaga Limestone. Because the Marcellus Shale is laterally widespread throughout the Appalachian Basin, variability in the thickness, thermal maturity, and pressure is common. Typically, the Marcellus Shale thickens from 0 feet in Ohio to more than 250 feet in Pennsylvania and New York. Wells targeting the Marcellus Shale are drilled to more than 5,000 ft with shallower wells in Ohio. Thermal maturity increases from east to west across the Appalachian Basin (Wrightstone, 2009). Operators report normal to above-normal pressure in the Marcellus Shale across the Basin. However, below-normal pressures have been reported in West Virginia, leading to alternative treatment parameters (Wrightstone, 2009). As with all unconventional reservoirs, production of the Marcellus Shale is directly related to the presence of natural fractures and the ability to stimulate those fractures during treatment.

Two fracture sets are present in the Marcellus Shale, as seen in Figure 2. J1 fractures are oriented northeast to southwest and were formed as natural hydraulic fractures during the Alleghenian Orogeny (Engelder et al., 2009). These fractures are parallel to the current maximum horizontal stress orientation in the Appalachian Basin. J2 fractures were formed during hydrocarbon generation and cross-cut the older J1 fracture set (Duncan and Williams-Stroud, 2009). J2 fractures are oriented northwest to southeast. Both J1 and J2 fracture sets are natural hydraulic fractures and have very similar apertures and surface roughness. However, the J1 fracture set lacks cement or mineralization due to the presence of methane which inhibits precipitation in the fractures (Engelder et al., 2009). The J1 fracture set is more prevalent and closely spaced than the J2 fracture set, which, combined with the lack of cement, yields a higher permeability for these fractures (Loewy, 1995; Lash et al., 2004; Kranz et al., 1979). Ideally, a horizontal well attempting to produce from the Marcellus Shale should activate the J1 fracture set to exploit the high permeability of these fractures and activate the J2 fractures to connect parallel J1 fractures. If the J2 fracture sets are stimulated, those fractures will inevitably intersect the J1 fracture set allowing production from those fractures. Operators drilling in the Marcellus Shale have found that well azimuths at a high angle to SHmax activate both the J1 and J2 fracture sets and yield the highest production.

Integrated Analysis

The microseismic response of the formation to the hydraulic stimulation of the five wellpads investigated in this publication shows considerable variation, as seen in Figure 3. Pronounced linear features can be observed in both the J1 and J2 direction, as well as larger linear structures extending over multiple wellbores at a slightly different azimuth, interpreted to be faults, as shown in Figure 4. Considering the regional geology and Marcellus-specific features, the recorded microseismic activity can be closely linked to the reactivation of natural fractures (Neuhaus et al., 2012).

Due to the wide azimuth, large aperture, and high fold geometry of the monitoring array, the seismic wavefront arriving at the receivers can be inverted for the focal mechanism of a microseismic event. For the data set presented in this publication, hundreds of source mechanisms have been picked, falling into four general groups. As illustrated in Figure 5, dip-slip, oblique dip-slip, strike-slip, and oblique strike-slip mechanisms were observed. Focal mechanisms do not only indicate the direction of movement along the failure plane, they also indicate the

stress state that facilitated the failure. Figure 6 shows the Andersonian faulting states for dip-slip and strike-slip failure. Dip-slip failure occurs in a normal faulting regime in which the overburden stress is the maximum principal stress, the maximum horizontal stress is the intermediate principal stress, and the minimum horizontal stress is the minimum principal stress. In a strike-slip faulting regime on the other hand, the maximum horizontal stress is the maximum principal stress, the vertical stress the intermediate principal stress, and the minimum horizontal stress remains the least principal stress (Neuhaus et al., 2012).

From the large population of focal mechanisms, the magnitudes and directions of the three principal stresses can be inverted. As dip-slip and strike-slip events are an indication of different stress regimes, the stress inversion was performed separately on these two groups of events. For every mechanism group, the direction of maximum horizontal stress as well as a stress ratio relating the three principal stresses to each other was calculated. The minimum horizontal stress was estimated from closure pressure analysis with treatment pressure data. Converting surface data to bottomhole data by accounting for rate-dependent friction pressure, closure pressure was determined for 25 stages with an overall average of 6,618 psi. Vertical stress was estimated at 7,090 psi by integrating a density log for an offset well under the array to the average target depth of all five well pads. The vertical stress and the maximum horizontal stress change places as maximum and intermediate principal stress for the two failure regimes and the stress ratio can be solved for both stress conditions.

The results can be seen in Table 1 illustrating the difference in maximum horizontal stress between the normal faulting regime and the strike-slip faulting regime. This is "a quantitative measure of the effect that the injection of treatment fluid and proppant has on the local stress state. The fact that the stress regime is different for microseismic events caused by dip-slip failure from events originating from points of strike-slip failure indicates that the additional pressure that the reservoir is subjected to during the injection is transmitted differently in different parts of the reservoir" (Neuhaus et al., 2012). Evaluating the occurrence of events in time with respect to their distance from the wellbore it was observed that the two mechanism groups define spatial and temporal subsets. The occurrence of dip-slip events peaks both closer to the wellbore and earlier in the stage, whereas the occurrence of strike-slip events peaks further away from the wellbore and later on in the stage (Williams-Stroud et al., 2012).

It is evident that a different local stress state is required for the occurrence of strike-slip events compared to dip-slip events. While the way the additional pressure the reservoir is subjected to during the injection is largely dependent on regional geology and the tortuous flowpath through the rock, stimulation approach also seems to have an effect. The way in which pressure in the reservoir along the wellbore is built up appears to be correlated to the occurrence of strike-slip events. Comparing conventional toe-to-heel one-well-at-a-time treatments to zipper-frac stimulations, the latter show almost twice as many strike-slip events. The average percentage of strike-slip events for the first case is 21% whereas the average for zipper-frac'ed wellbores is 38%. Relating the percentage of strike-slip events to production normalized by lateral length, Neuhaus et al. (2012) showed that there is a weak positive correlation between the two. The relevance of this becomes obvious when examining the natural fracture reactivation visible in the data set.

Although both dip-slip and strike-slip failure occur along both joint sets, it was observed that strike-slip events tend to form lineaments in the J2 direction substantially more pronounced than in the J1 direction; dip-slip events showed the opposite behavior. More strike-slip failure might therefore be an indication of increased J2 reactivation. Since two joint sets are found in the Marcellus, it might be beneficial for a stimulation treatment to reactivate both in order to increase the complexity of the fracture network and subsequently enhance the overall

permeability of it. Due to the local in-situ stress state and stress-dependent permeability, flow in the J1 direction might be preferred over flow in the J2 direction but J2 joints connecting the almost perpendicular J1 joints might be beneficial regardless.

Modeling

A discrete fracture network (DFN) was generated using information from the microseismicity as well as outcrop information about natural fractures in the Marcellus Shale representing the unstimulated background network in the reservoir. The orientation of the fracture failure plane was defined using data from the source mechanisms with a statistic scatter applied to it where the orientation maximum is centered on the focal mechanisms failure plane. The size of the fractures was dependent on the relative energy of the events within a geologically reasonable length range and a length to height aspect ratio of 2:1. Figure 7 shows the DFN with J1 and J2 joints, as seen in the outcrop and from the microseismicity. A DFN-based hydraulic fracture simulation program was then used to model the reactivation of natural fractures in the DFN due to the injection. Using the stress parameters obtained from the treatment pressure analysis and the stress inversion, a series of simulations were run to calculate where failure should occur on fractures in the DFN; this was based on a Mohr-Coloumb criterion determining where stress conditions are met that cause slip on the fracture face. A base case model was created that matched the observed reactivation of natural fractures seen in the microseismicity by adjusting certain input values within a reasonable range. Figure 8 shows reactivation of both the J1 and the J2 joints in the model. The growth extending from the wellbore follows the J1 fractures roughly parallel to the direction of maximum horizontal stress with the J2 joints connecting the longer J1 trends to each other.

The in-situ stress state that was determined to be present at the beginning of the treatment was used in the model as a static condition; the maximum principal stress is vertical. While the microseismic data also shows the presence of a strike-slip faulting regime on a very local scale, the modeled reactivation of both joint sets for the base case model suggests that the fluid pressure increase during the treatment is high enough to already cause failure along joints that strike at a very high angle to the maximum horizontal stress for the normal faulting regime.

Treatment Optimization

Using the base model DFN for the Marcellus case study, we explore the effect of changes in treatment parameters on the resulting fracture network for three consecutive stages on one of the wellbores included in this study. Ultimately, we hope to refine completions designs for optimal economic return. We selected five treatment attributes and re-ran the DFN model; varying a single attribute for each run.

Flow Rate

The flow rate of the treatment fluid was allowed to vary +/– 30% from the base model. The resulting DFN models are shown in Figure 9 (left) the reduced case, and Figure 9 (right) the increased case.

The lower flow rate DFN model returns a much smaller fracture network due to the lower volume of fluid injected and the lower energy content of the injection associated with the lower flow rate. When the flow rate was increased, the model developed an area of aggressive fracturing and a less complex fracture network than the base model. The greater momentum of the fluid that is associated with an increased pump rate can

make it more difficult for the fluid to turn corners. Fractures in the increased flow rate model align strongly with SHmax.

Pressure

The treatment pressure in the model was also varied up to 30%. The resulting DFN models are shown in Figure 10 (left) reduced treatment pressure and Figure 10 (right) increased treatment pressure.

The injection pressure is an indication of the ease with which the reservoir takes fluid. A lower treatment pressure represents a condition where the fluid can move more easily around the tortuous reservoir. The lower pressure model therefore shows fluid following paths of least resistance. Natural fractures and thief features allow fluids to flow far afield without creating additional permeability. The increased pressure model indicates greater resistance to injection. This result is a function of the rock properties incorporated into the model. The results do not seem to represent a real case where increased pressure is tied to an increase in fluid flow rate. This result indicates that the idea of establishing pressure as the only variable in the model is inaccurate. Pressure change is intrinsically tied to flow rate and cannot be accurately modeled separately.

Duration

The duration of treatment was allowed to vary by +/– 30%. The resulting DFN models are shown in Figure 11 (left) shorter duration and Figure 11 (right) increased duration.

Increasing the duration of the treatment also means increasing the volume of fluid while maintaining the flow rate at the base case level. When duration was decreased, the fracture network model was diminished, as expected. The opposite is true for increasing treatment duration. Microseismic evidence suggests there is a point of diminishing returns in stage treatment duration. The outside edge of the treatment fluid continues to expand into the reservoir, decreasing pressure per square inch as it grows. When the fracture network is too large at the outer edge, the pressure at the fracture tips is not sufficient to continue fracture propagation.

Stage Length

Stage length was varied by +/– 20 feet for the reduced and increased models while maintaining the distance between stages. The resulting DFN models are shown in Figure 12 (left) shorter stage length and Figure 12 (right) longer stage length.

The difference between the reduced stage length case and the extended stage length case is not significant enough to establish a marked difference within the modeling software. It was expected that longer stages reduce cluster density, showing less interference between the fractures growing from each cluster. Closer cluster spacing with a highly dense natural fracture network, as is present in Marcellus, is expected to create a more complex network. If an increased stage length produced a sufficiently complex fracture network, one stage over the length of the wellbore could be eliminated resulting in substantial savings per well pad.

Number of Perforations

The number of perforations was allowed to vary +/- one extra perforation holding the perforation interval fixed. The resulting DFN models are shown in Figure 13 (left) fewer perforations and Figure 13 (right) more perforations.

Based on the models run, an increased number of perforations cause overlap and interference of stimulated fracture zones. In a reservoir where the natural fracture network is already dense (as the Marcellus), the increased number of perforations increased reactivation of the J1 and J2 joints creating a more interlinked fracture network than the base model. Decreasing the number of perforations, in this Marcellus case study, lead to less reactivation of natural fractures; the model shows a less desirable outcome than the base model.

Discussion

In the Marcellus Shale a calibrated DFN model was used as the basis for exploring well treatment parameters. Five well treatment attributes (flow rate, treatment pressure, stage duration, stage length, number of perforations, and perforation cluster spacing) were varied to investigate the optimum range for each factor.

The increased flow rate model showed better results than the reduced flow rate model. Given the possibility of overstimulation, considering the wellbore spacing in the study, the increased flow rate model is not clear enough to make a definitive recommendation. An increased flow rate might also result in additional operational effort such as higher hydraulic horse power requirements, which together with the cost increase due to pumping more material might not yield the required improvement to make it an economically feasible option.

The lower pressure model showed better results than the increased pressure model. However, the modeled treatment pressure is not tied to a flow rate that can be realized. No recommendation can be made based on these results.

The longer duration treatment model outperformed the short duration model. Given the wellbore spacing of the modeled location, longer duration leads to overstimulation (i.e. too much overlap onto the neighboring wellbores). The economic trade off depends on the well spacing of a planned field versus the expense of pumping resources.

Stage length poses the most cost saving attribute of all of the models considered in this study. Unfortunately, the model results were not conclusive enough to make a strong recommendation. Increasing the number of perforations resulted in a better fracture network model than the reduced number. Compared to the base case, the improvement is minor and might not warrant the cost of an additional perforation cluster. The operational costs associated with an additional perforation cluster probably do not justify the expense.

Theoretically, of all completion parameters that were varied, the one that would result in the most savings is increasing the stage length. Increasing or decreasing the stage by 20 ft was chosen as it would result in either saving one stage or adding one over the total length of the wellbore. Given the natural fracture density observed in outcrops of the Marcellus Shale, an additional five feet between each of the five perforation clusters (due to eliminating one stage) should only minutely change the hydraulic fracture network. Especially since J1 fractures are

so dense and closely spaced that virtually no difference should be observed while costs could be reduced as well as the environmental footprint of the treatment. If one hydraulic fracturing stage per well could therefore be eliminated, the potential savings for an entire well pad can approach a seven figure dollar amount. Unfortunately the model was not conclusive enough to make a definitive call.

Further studies could be conducted using a more sophisticated model where attributes are fully dependent on each other. An increasing treatment pressure, for example, should be coupled to a change in flow rate. Additionally, although Neuhaus et al. (2012) showed that the observed microseismic activity is related to the reactivation of natural fractures, some emphasis should be put on the induced hydraulic fracture in future modeling efforts.

Conclusion

An integrated analysis of hydraulic fracturing treatments in the Marcellus Shale monitored by a permanently installed array of buried geophones was conducted to investigate the relationship between reservoir geology, wellbore completion and stimulation design, and microseismic data. A calibrated DFN model was used as the basis for exploring well treatment parameters. Five well treatment attributes (flow rate, treatment pressure, stage duration, stage length, number of perforations, and perforation cluster spacing) were varied to investigate the optimum range for each factor. Varying stage length shows the highest potential in cost savings by eliminating only one stage per well. The investigation conducted in this study illustrated that while an increased stage length resulted in a fracture network very similar to the base case model suggesting a similar treatment efficiency over the length of the wellbore, this observation was not conclusive enough as a decreased stage length produced a very similar result.

Acknowledgments

The authors would like to thank Gastar Exploration Ltd. for generously agreeing to publish the findings of this study. Furthermore, they would like to express their gratitude to MicroSeismic, Inc. for providing time and resources to conduct this case study.

References Cited

Duncan, P.M., and S. Williams-Stroud, 2009, Marcellus Microseismic: Oil and Gas Investor, v. 10, p. 65-67.

Engelder, T., G.G. Lash, and R.S. Uzcategui, 2009, Joint sets that enhance production from Middle and Devonian gas shales of the Appalachian Basin: AAPG Bulletin, v. 93/7, p. 857-889.

Kranz, R.L., A.D. Frankel, T. Engelder, and C.H. Scholz, 1979, Permeability of whole and jointed Barre granite: International Journal of Rock Mechanics and Mining Sciences and Geomechanics Abstracts, v. 16, p. 225-234.

Lash, G.S., S. Loewy, and T. Engelder, 2004, Preferential jointing of Upper Devonian black shale, Appalachian Plateau, U.S.A.: Evidence supporting hydrocarbon generation as a joint-driving mechanism: Geological Society Special Publications, 231, p. 129-151.

Loewy, S.L., 1995, The post-Alleghenian tectonic history of the Appalachian Basin based on joint patterns in Devonian black shales: M.S. Thesis, Pennsylvanian State University, University Park, Pennsylvanian, p. 179.

Neuhaus C.W., S. Williams-Stroud, C. Remington, W.B. Barker, K. Blair, G. Neshyba, and T. McCay, 2012, Integrated Microseismic Monitoring for Field Optimization in the Marcellus Shale: SPE Canadian Unconventional Resources Conference, Calgary, AB, Canada, SPE 161965, 16 p.

Williams-Stroud, S., C.W. Neuhaus, C. Telker, C. Remington, W.B. Barker, G. Neshyba, and K. Blair, 2012, Temporal Evolution of Stress States from Hydraulic Fracturing Source Mechanisms in the Marcellus Shale: SPE Canadian Unconventional Resources Conference, Calgary, AB, Canada, SPE 162786, 6 p.

Wrightstone, G., 2009, Marcellus Shale – Geologic Controls on Production: AAPG Search and Discovery Article #10206. Website accessed 26 July 2013. http://www.searchanddiscovery.com/documents/2009/10206wrightstone/index.htm

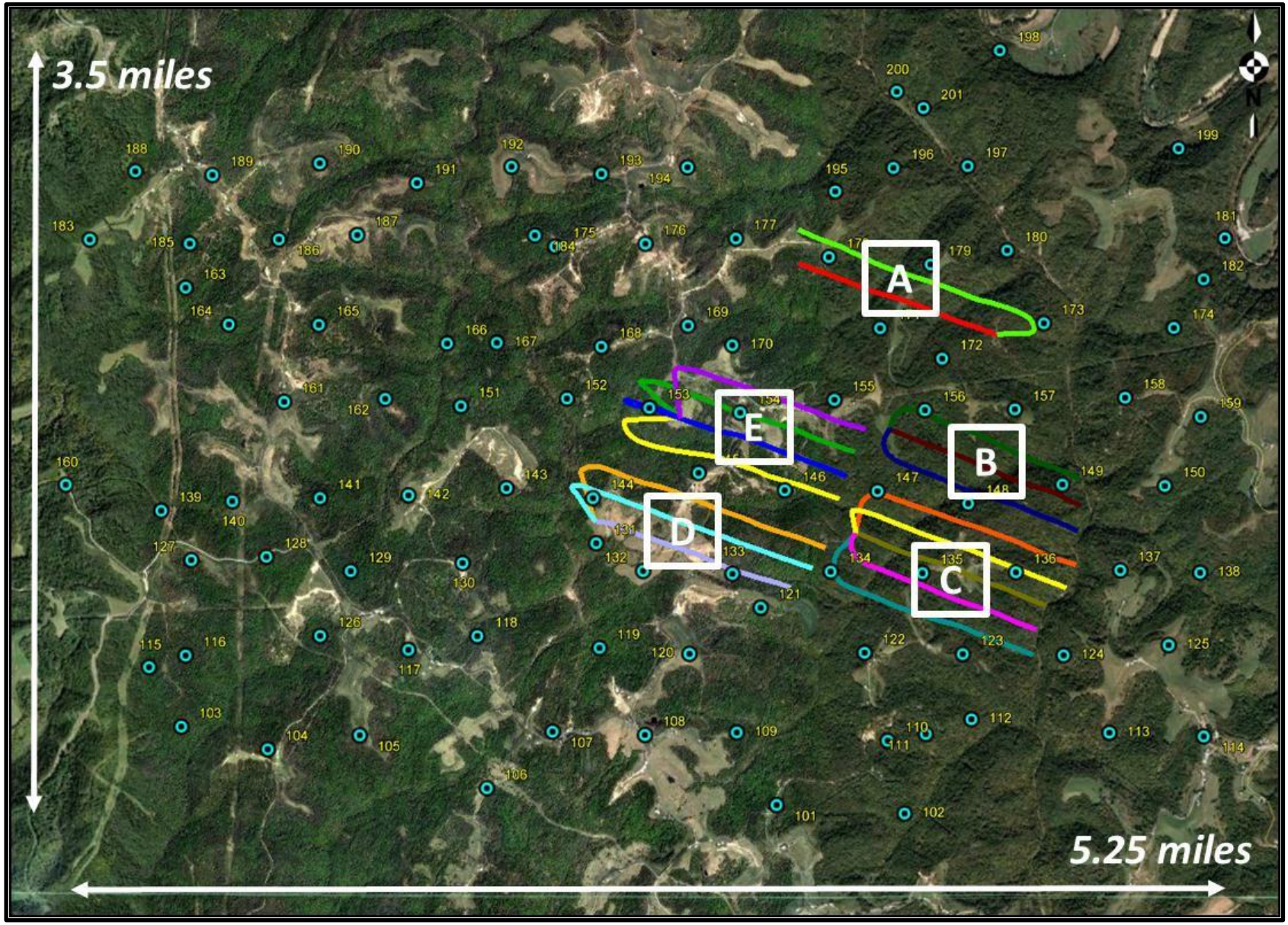

Figure 1. Map view of surface microseismic monitoring array. Recording stations can be seen as turquoise circles. Wellpads are named with letters.

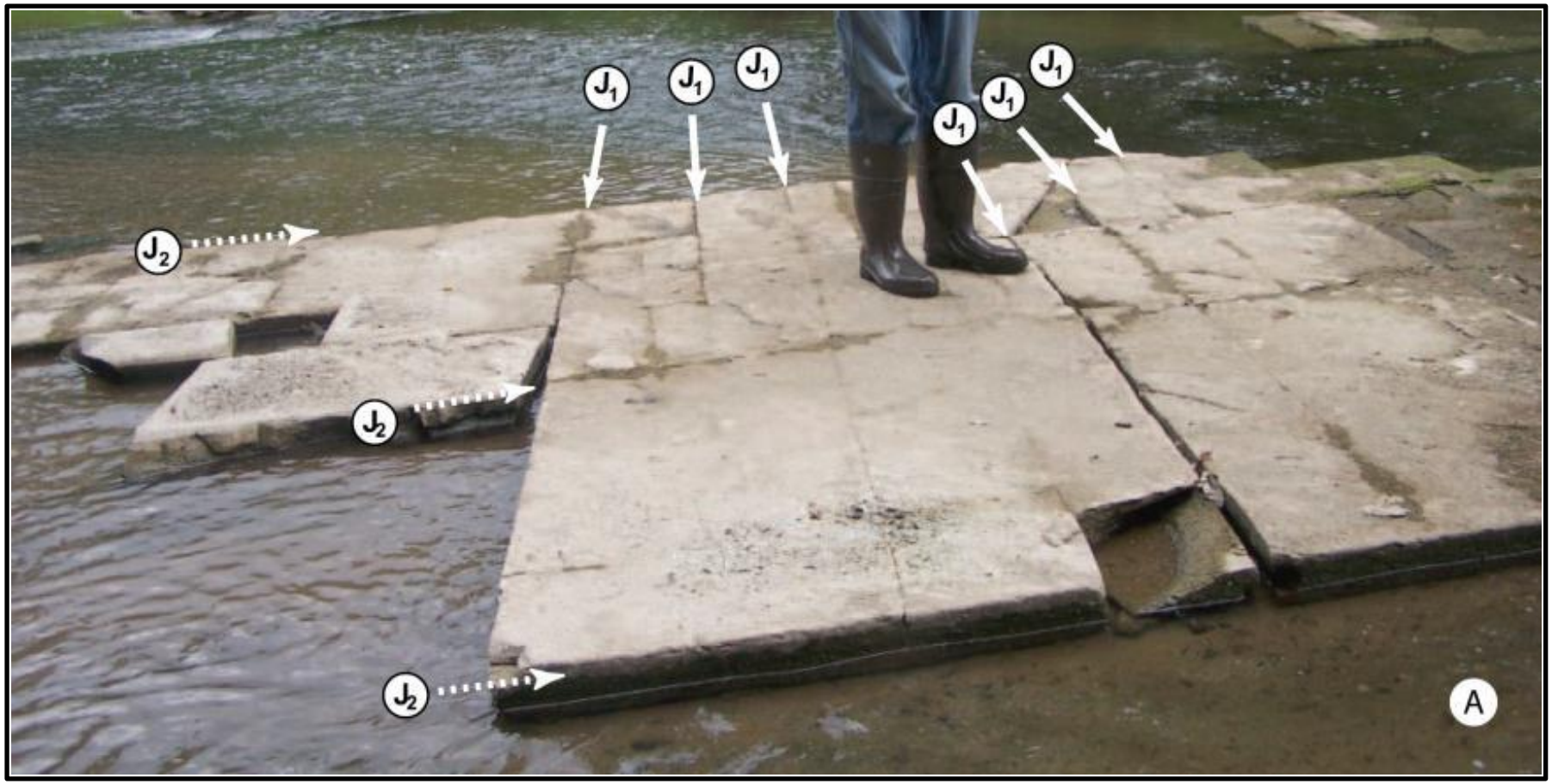

Figure 2. Marcellus joint sets (from Engelder et al., 2009).

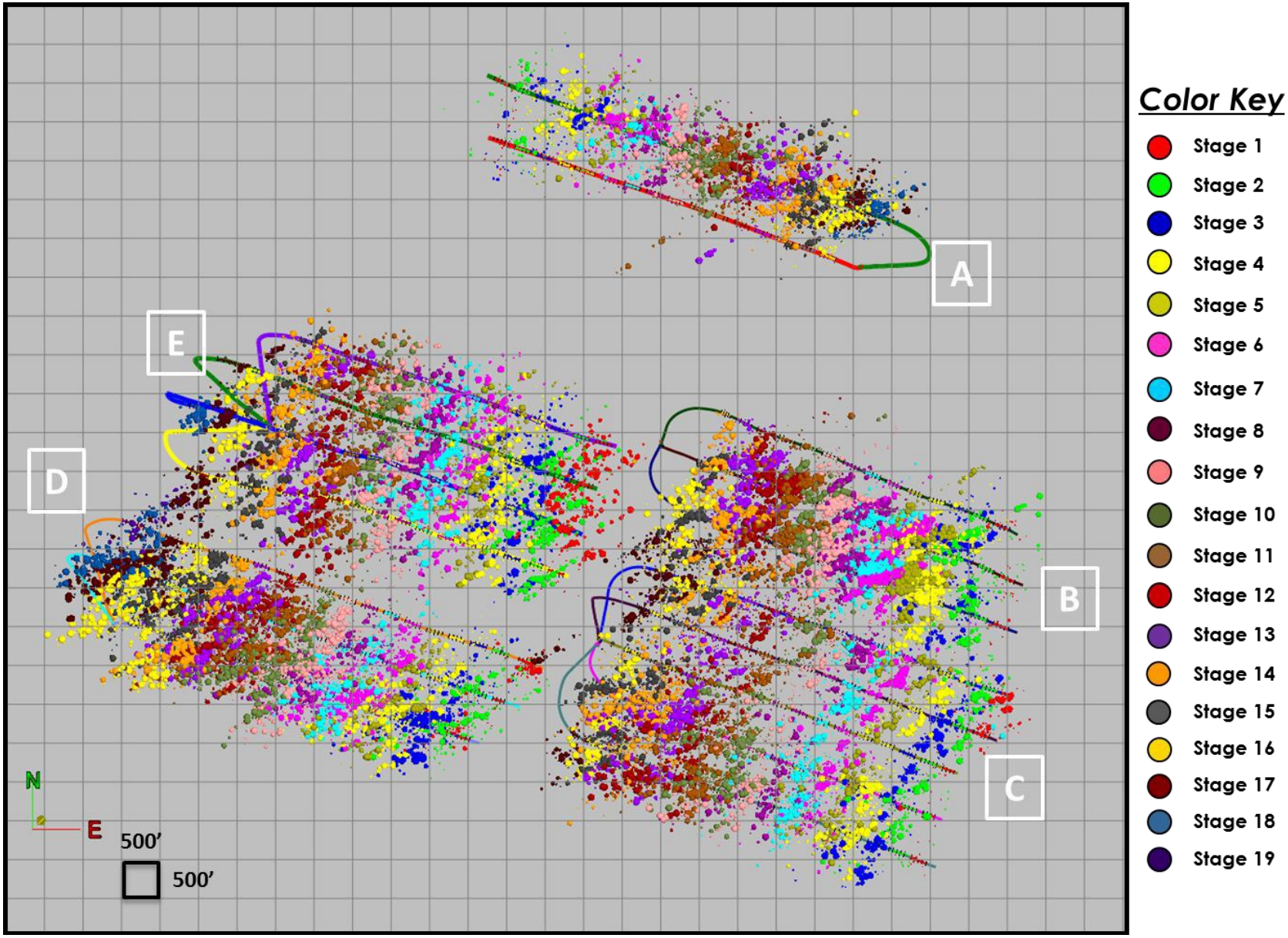

Figure 3. Map view of microseismic events for Marcellus case study. Events are colored by stage and sized by energy.

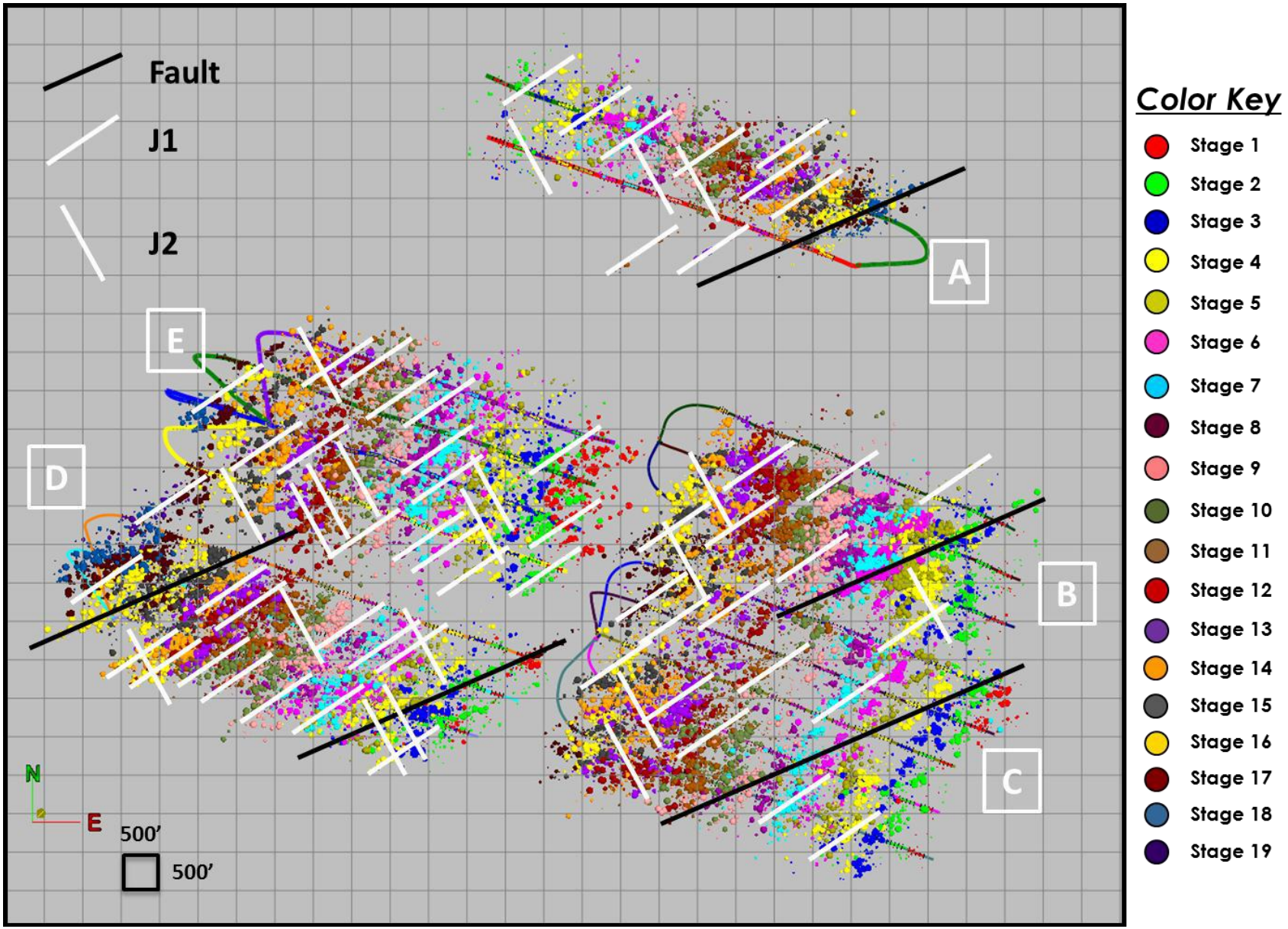

Figure 4. Map view of microseismic events for Marcellus case study. Events are colored by stage and sized by energy. Fault, J1, and J2 features are visible in the data and illustrated by lines with respective color and orientation.

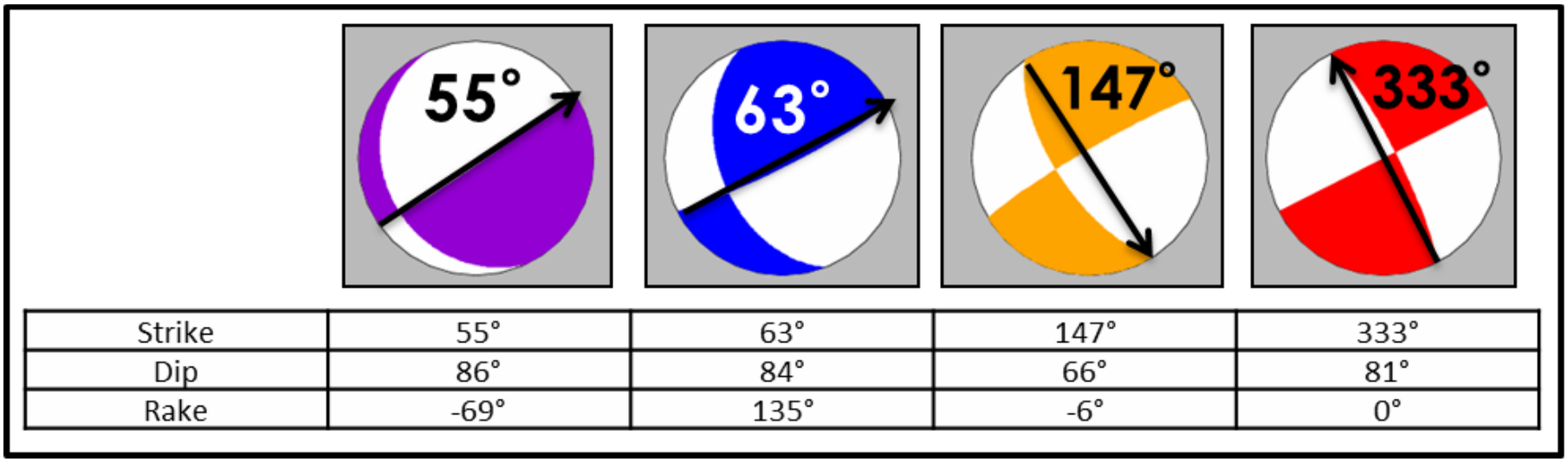

Strike	55°	63°	147°	333°
Dip	86°	84°	66°	81°
Rake	-69°	135°	-6°	0°

Figure 5. Focal mechanisms.

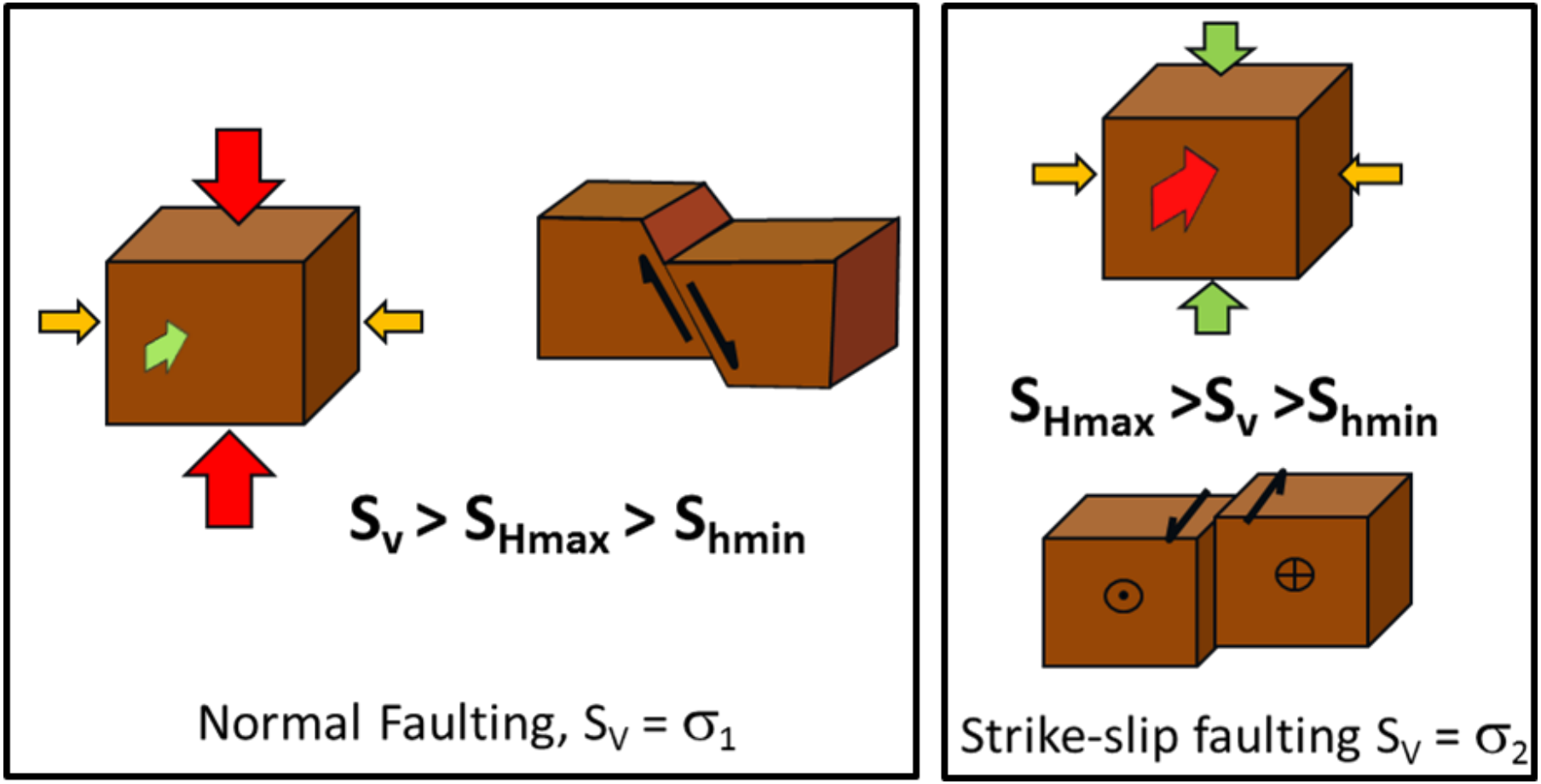

Figure 6. Andersonian faulting states. The colored arrows indicate the principal stresses. Red represents the maximum principal stress, green the intermediate principal stress, and orange the minimum principal stress.

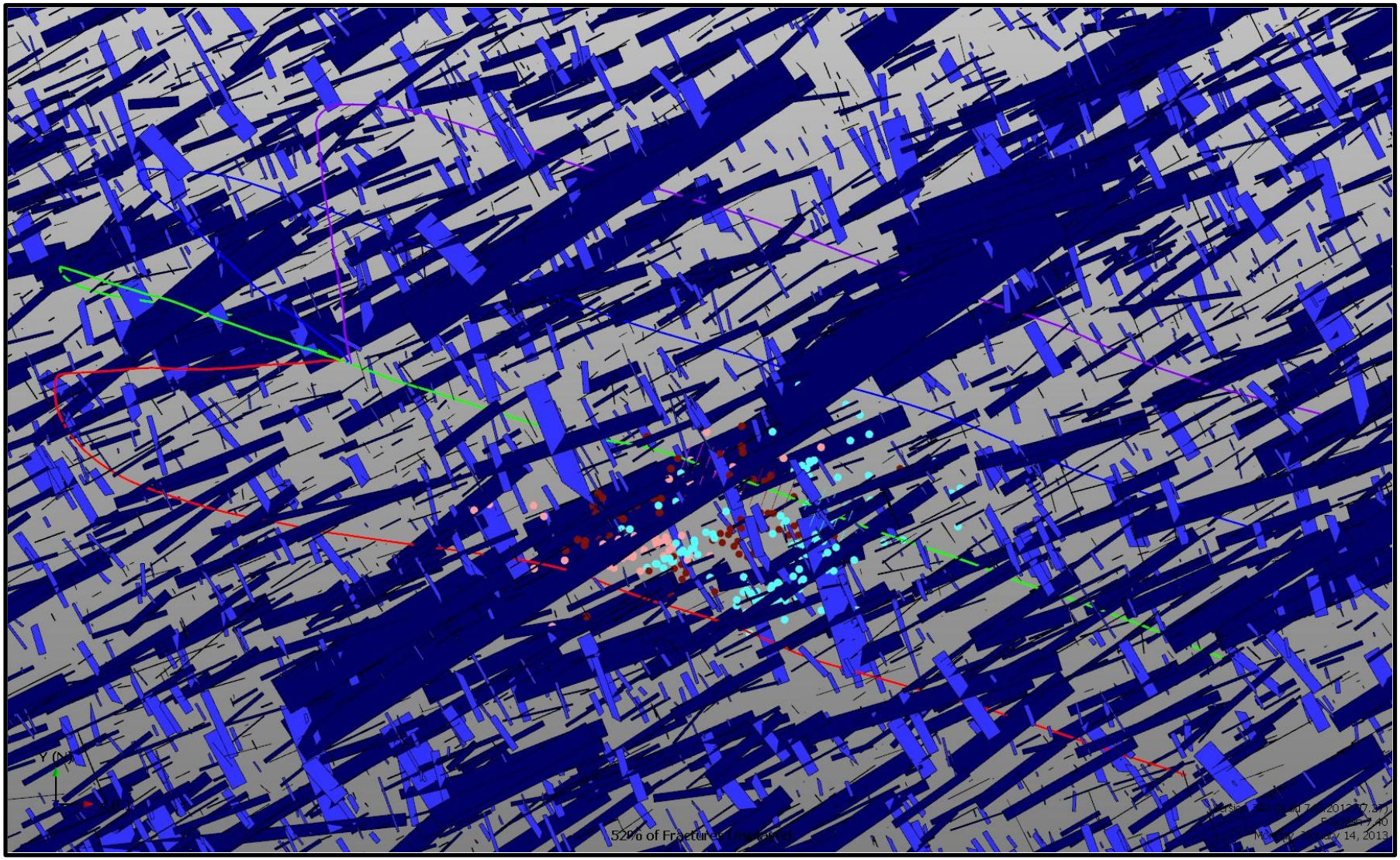

Figure 7. Map view of the DFN model representing the unstimulated natural fracture network in the Marcellus. J1 joints can be seen in the northeast-southwest direction with J2 joints shown in the northwest-southeast direction. Due to the high fracture density only 10% of the fractures are displayed. This model was the base case model for treatment optimization modeling. The contiguous lines represent wellbores. The microseismic data is shown as colored dots; the discs on the wellbore are individual perforation intervals. Fracture planes are shown in green.

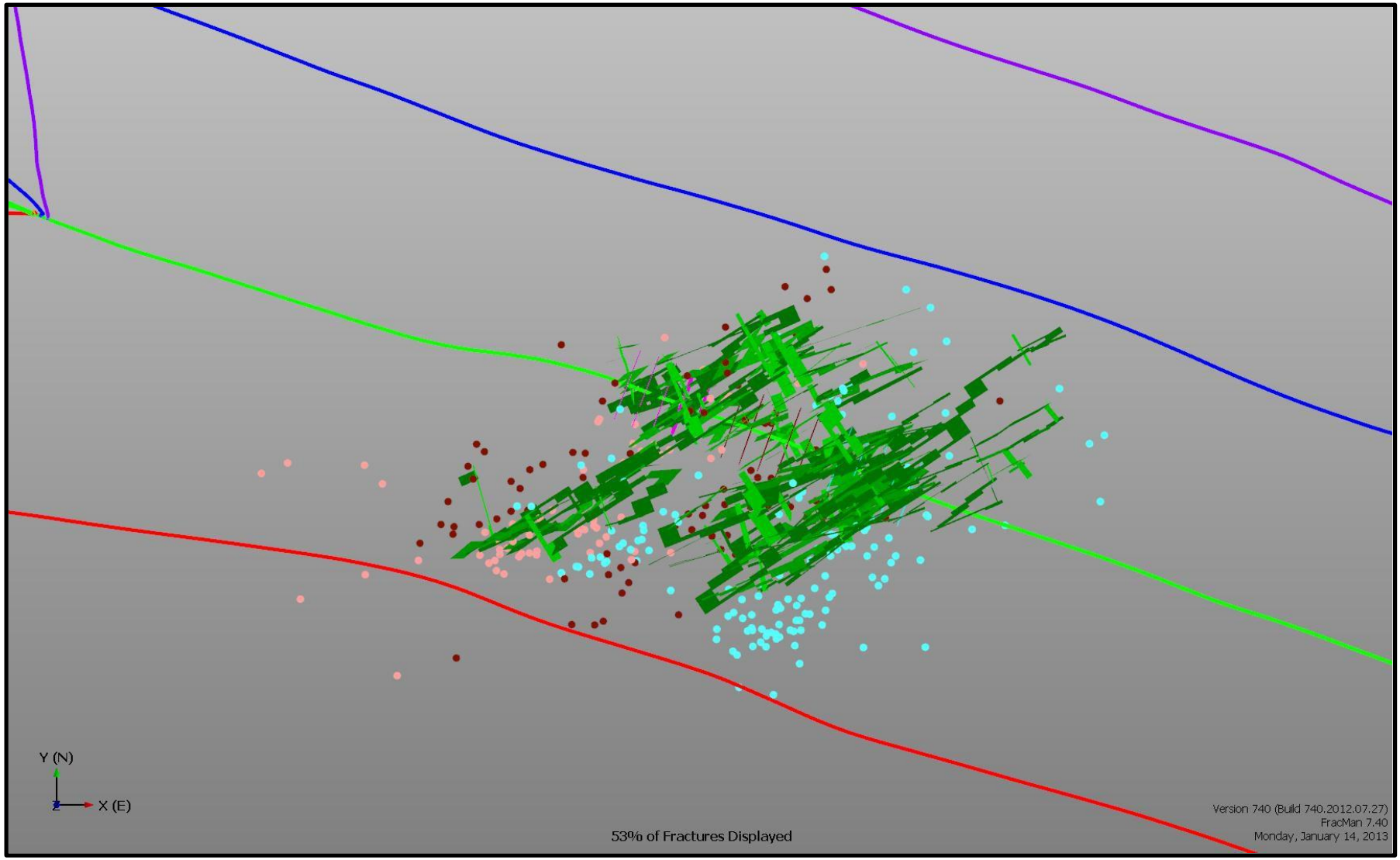

Figure 8. Map view of the base case model of the reactivated natural fractures during stimulation used for treatment optimization modeling. The contiguous lines represent wellbores. The microseismic data is shown as colored dots; the discs on the wellbore are individual perforation intervals. Fracture planes are shown in green.

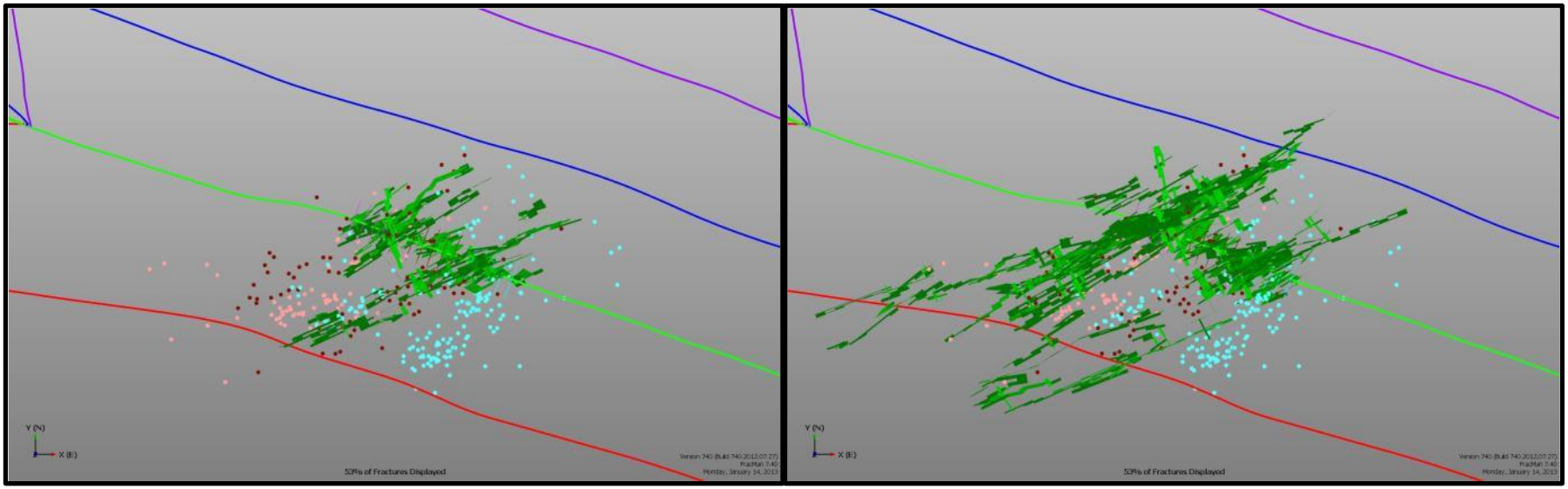

Figure 9. Map view of DFN model with lower (left) and increased (right) treatment flow rate. The contiguous lines represent the wellbores. The microseismic data is shown as colored dots; the discs on the wellbore are individual perforation intervals. Fracture planes are shown in green.

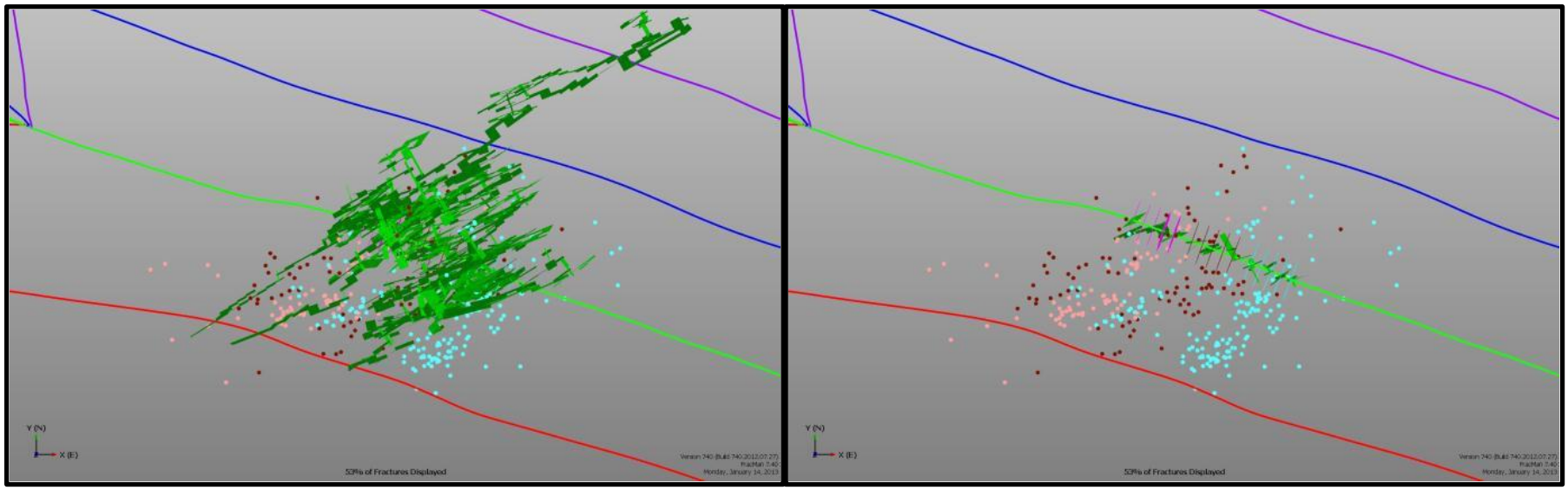

Figure 10. Map view of DFN modeled with lower (left) and increased (right) treatment pressure. The contiguous lines represent the wellbores. The microseismic data is shown as colored dots; the discs on the wellbore are individual perforation intervals. Fracture planes are shown in green.

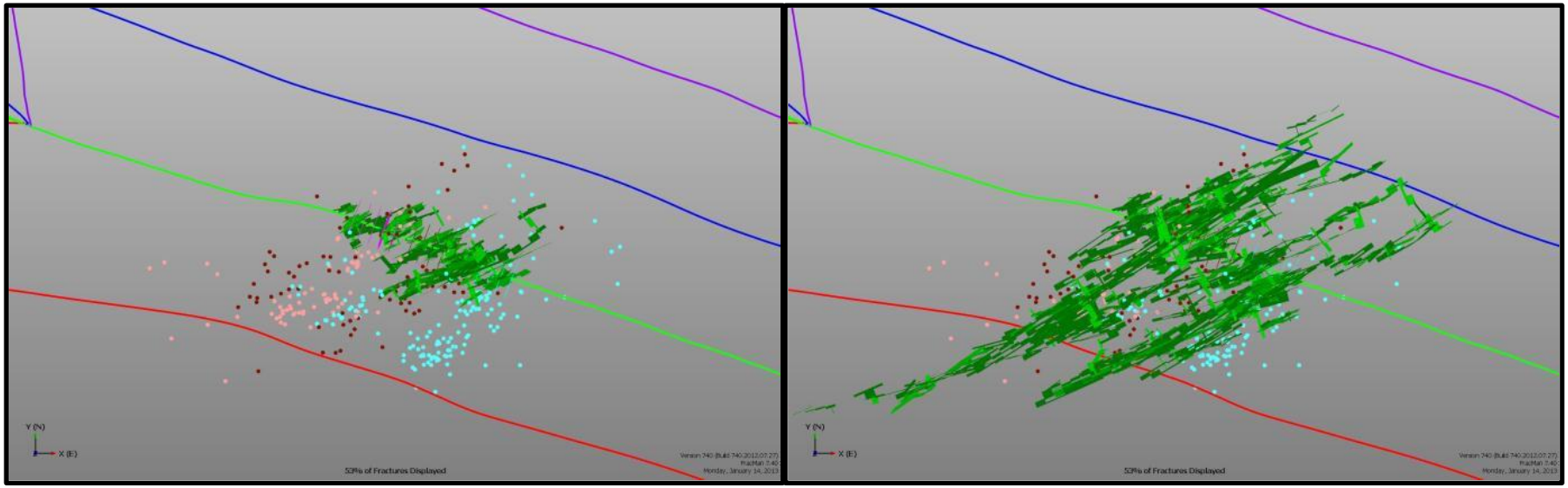

Figure 11. Map view of DFN model with shorter (left) and longer (right) treatment duration. The contiguous lines represent the wellbores. The microseismic data is shown as colored dots; the discs on the wellbore are individual perforation intervals. Fracture planes are shown in green.

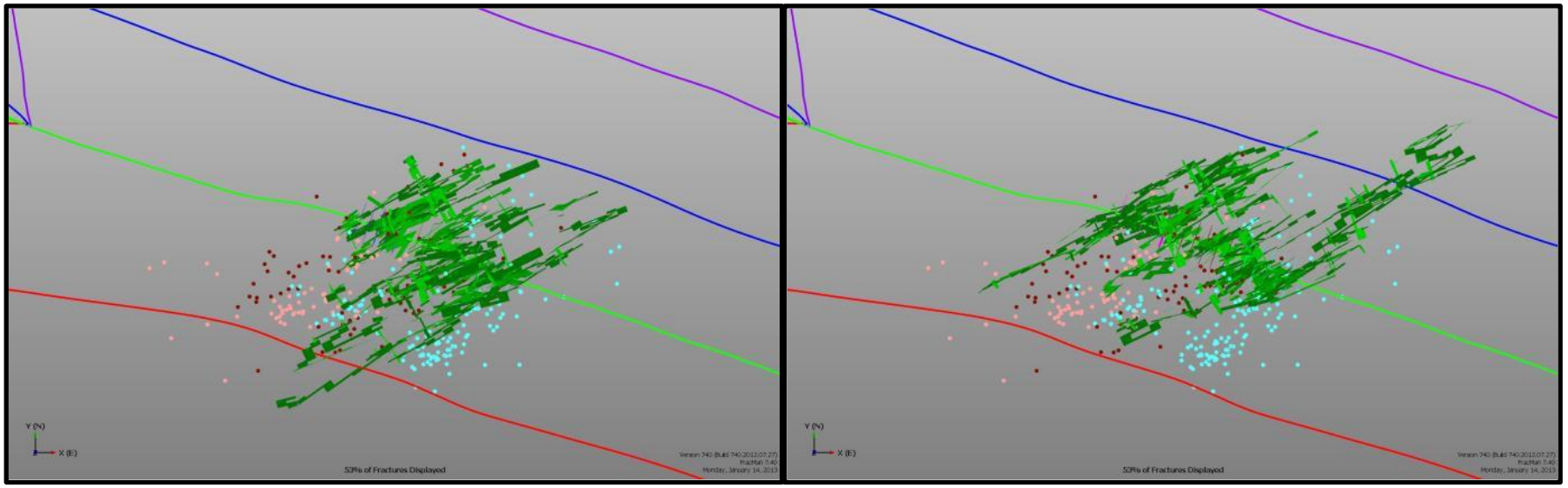

Figure 12. Map view of DFN model with decreased (left) and increased (right) stage length. The contiguous lines represent the wellbores. The microseismic data is shown as colored dots; the discs on the wellbore are individual perforation intervals. Fracture planes are shown in green.

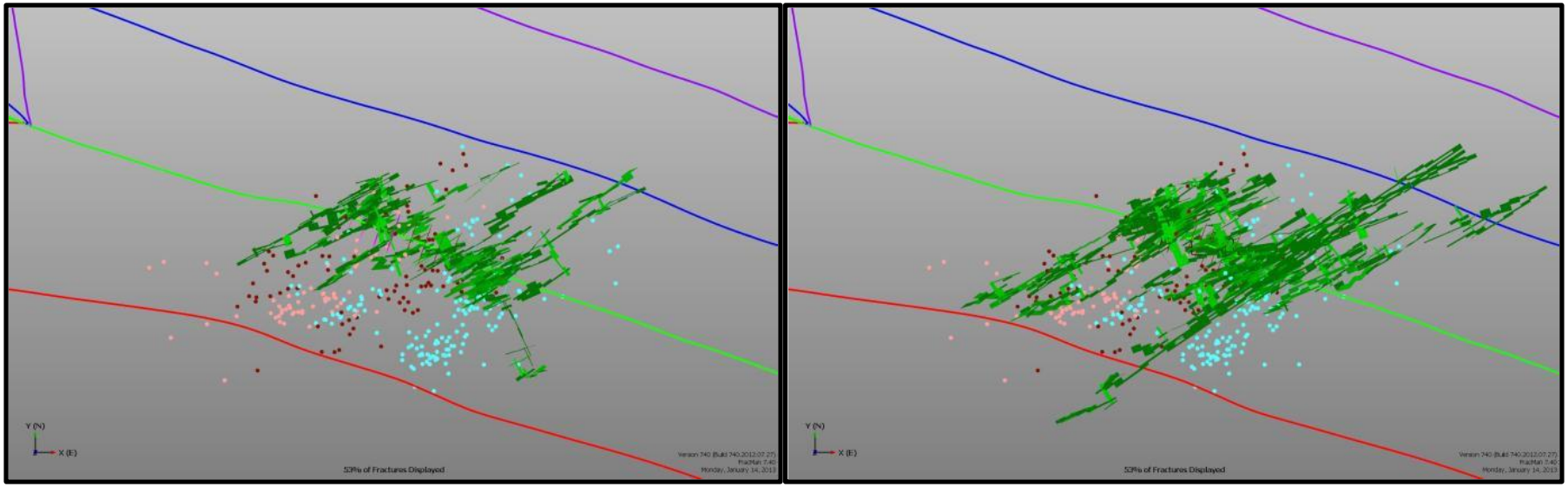

Figure 13. Map view of DFN modeled with fewer perforations (left) and more perforations (right). The contiguous lines represent the wellbores. The microseismic data is shown as colored dots; the discs on the wellbore are individual perforation intervals. Fracture planes are shown in green.

Regime	Φ	σ_1 [psi]	σ_2 [psi]	σ_3 [psi]	S_{Hmax} orientation
Dip-Slip	0.80	7,090 (Sv)	6,996 (S_{Hmax})	6,618 (S_{hmin})	Northeast-southwest
Strike-Slip	0.69	7,302 (S_{Hmax})	7,090 (Sv)	6,618 (S_{hmin})	Northeast-southwest

Table 1. Principal stresses for failure regimes.